Multi-frequency EPR for Transition Metal Ions

Alexander Schnegg

Max Planck Institute for Chemical Energy Conversion

The EPR Research Group @ MPI for Chemical Energy Conversion

EPR for Catalysis Research

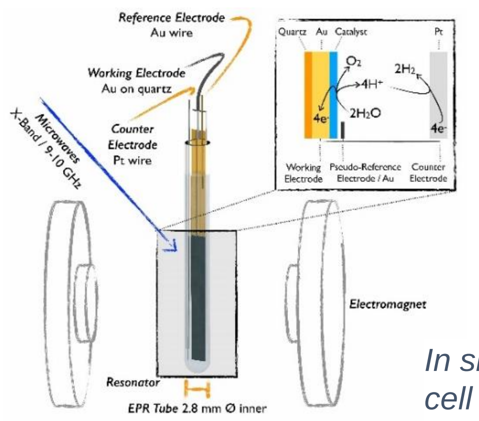

Sonia Chabbra

Shannon Bonke

In situ electrochemical cell integrated in an EPR spectrometer.

High resolution EPR on metal proteins

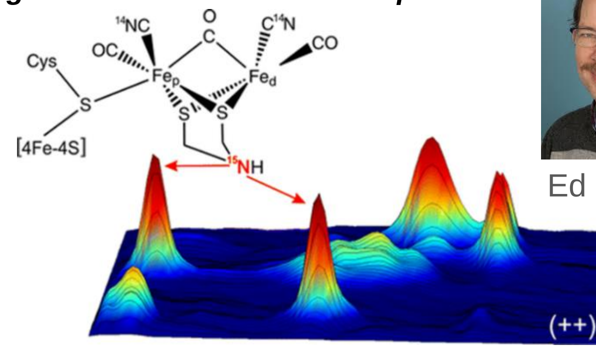

Ed Reijerse

Leonid Rapatskiy

Hyperfine sublevel correlation spectroscopy on the H-cluster with ^{15}N enriched ADT amine. http://dx.doi.org/10.1039/c4cp05426a

Novel EPR detection schemes

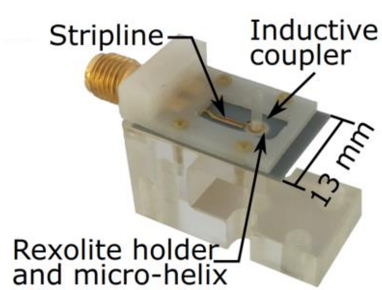

Jason Sidabras

Markus Teucher

-band EPR micro resoantor for protein single X-tals

High-spin transition metal states

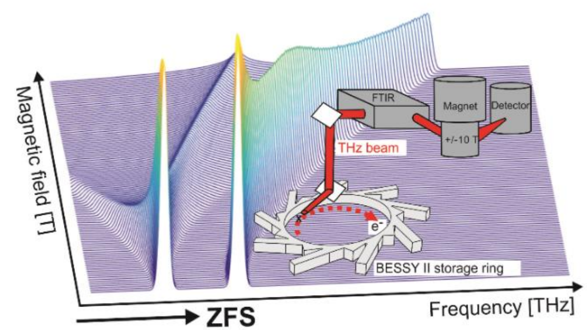

Joscha Nehrkorn

Thomas Lohmiller

2D EPR map for a S = 1 state with very large ZFS. Insert: THz-EPR spectrometer @ BESSY II.

Outline

- $S > 1/2$ transition metal ion states
- Zero field splitting – magnetic anisotropy
- Integer spin (non Kramers) and half integer spin (Kramers) system
- Weak-field and strong-field regimes
- Effective Spins and effective g-values of Kramers systems in the weak field regime.
- Multi-frequency EPR detection techniques

Systems with High Spin Transition Metal Ion States

Metalloproteins

Myoglobin structure

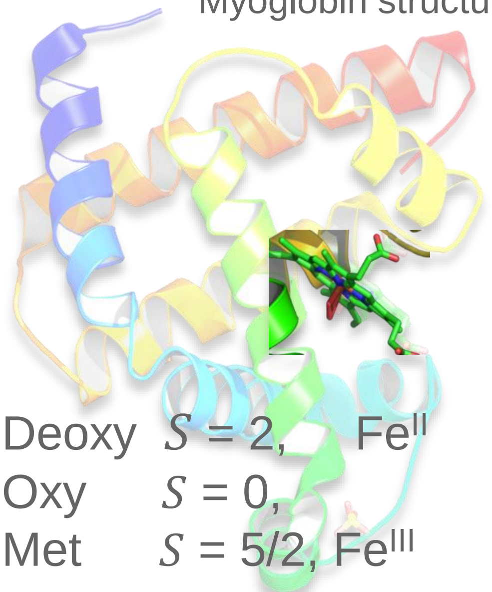

Deoxy $S = 2$, Fe^{II}
Oxy $S = 0$,
Met $S = 5/2$, Fe^{III}

Ingram, et al. ***Nature*****,** *178*, 4539, 905 (1956)

TMI catalysts

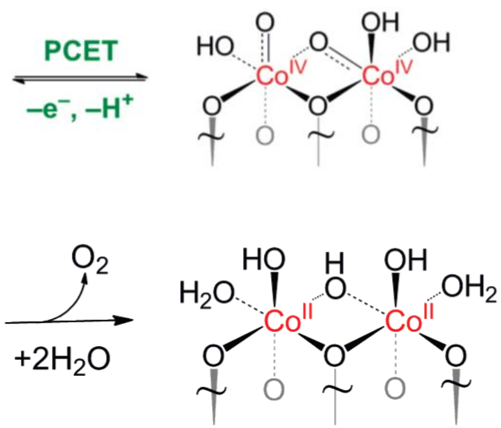

Nocera et al. , ***JACS***, 132, 16501 (2010)

Molecular Nanomagnets

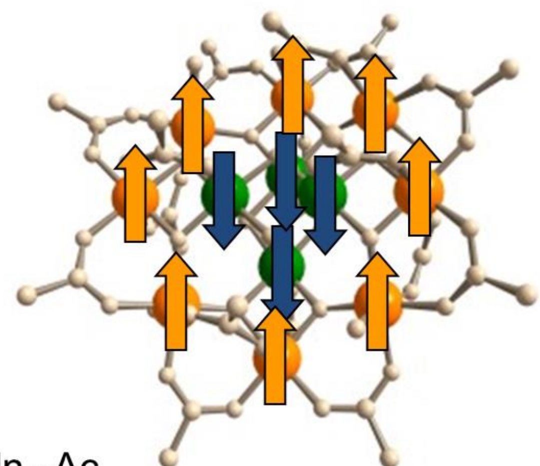

$Mn_{12}Ac$

Caneschi, et al. ***JACS,*** 113 *(15), 5873* (1991)

Probe electronic structure via ZFS.

➔ Understand and control (bio) catalytic properties.

Spin couplings determine magnetic properties
➔ Understand and control magnetic properties.

High Spin Transition Metal Ion States

- In EPR slang systems with $S > ½$ are referred to as high spin systems.
- $S > ½$ states originate from coupled electron spins.
- Total spin S is determined by Hund's rule.
  "For a given electron configuration, the term with maximum multiplicity ($2S + 1$) has the lowest energy."

Example Fe^{III} ($S = 5/2$)

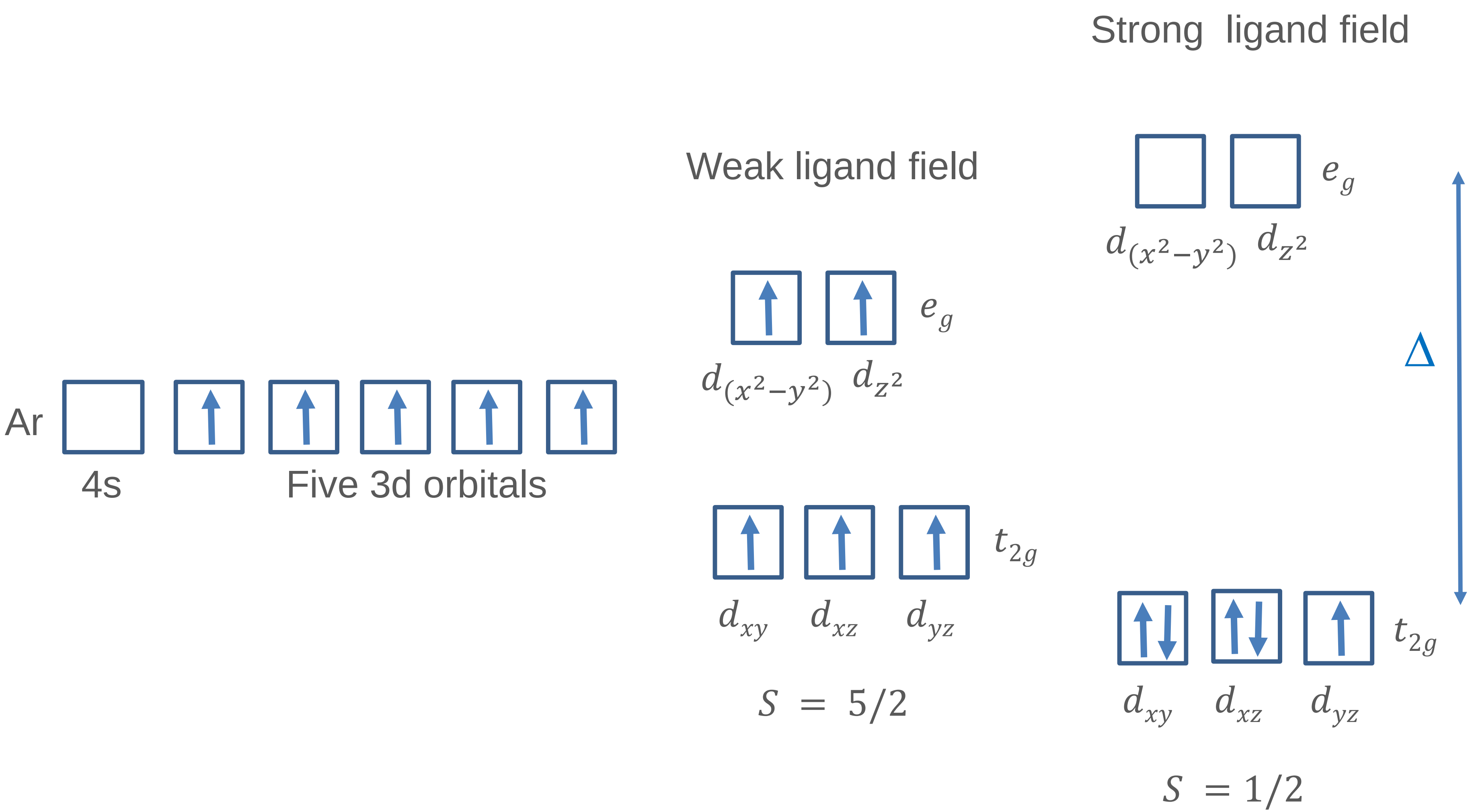

Octahedral coordination

Common EPR active 3d TMI States

3d¹	3d²	3d³	3d⁴	3d⁵	3d⁶	3d⁷	3d⁸	3d⁹	3d¹⁰	
_ _ ↑ _ _	_ _ ↑ ↑ _	_ _ ↑ ↑ ↑	↑ _ ↑ ↑ ↑	↑ ↑ ↑ ↑ ↑	↑ ↑ ↑↓ ↑ ↑	↑ ↑ ↑↓ ↑↓ ↑	↑ ↑ ↑↓ ↑↓ ↑↓	↑↓ ↑ ↑↓ ↑↓ ↑↓	↑↓ ↑↓ ↑↓ ↑↓ ↑↓	HS
Octahedral coordination		Δ	_ _ ↑↓ ↑ ↑	_ _ ↑↓ ↑↓ ↑	_ _ ↑↓ ↑↓ ↑↓	↑ _ ↑↓ ↑↓ ↑↓				LS
1/2	1	3/2	2 1	5/2 1/2	2 0	3/2 1/2	1	1/2	0	HS LS
			V^{I}	Cr^{I}	Mn^{I}	Fe^{I}	**Co^{I}**	**Ni^{I}**	Cu^{I}	
		V^{II}	**Cr^{II}**	**Mn^{II}**	**Fe^{II}**	**Co^{II}**	**Ni^{II}**	**Cu^{II}**		
Ti^{III}	**V^{III}**	**Cr^{III}**	**Mn^{III}**	**Fe^{III}**	Co^{III}	Ni^{III}	Cu^{III}			
V^{IV}	Cr^{IV}	**Mn^{IV}**	**Fe^{IV}**	Co^{IV}	Ni^{IV}					

High Spin Transition Metal Ion States

- In EPR slang systems with $S > ½$ are referred to as high spin systems.
- $S > ½$ states originate from coupled electron spins.
- Total spin S is determined by Hund's rule.
  "For a given electron configuration, the term with maximum multiplicity $(2S + 1)$ has the lowest energy."
- Systems with S > ½ exhibit an additional interaction
  – the Zero-Field Splitting (ZFS)
- ZFS leads to splitting of the spin energy levels without external magnetic field.

Spin Hamiltonian

Zeeman **Zero field splitting** **Hyperfine** **Spin-Spin Coupling**

$$\hat{\mathrm{H}} = \sum_j \left[\mu_\mathrm{B}\boldsymbol{B}_0\mathbf{g}_j\hat{\boldsymbol{S}}_j + \hat{\boldsymbol{S}}_j\mathbf{D}_j\hat{\boldsymbol{S}}_j\right] + \sum_j\sum_l \hat{\boldsymbol{S}}_j\mathbf{A}_{jl}\hat{\boldsymbol{I}}_l + \sum_j\sum_{j<k} J_{jk}\hat{\boldsymbol{S}}_j\hat{\boldsymbol{S}}_k$$

μ_B :Bohr magneton; $\boldsymbol{B}_0$**:** external magnetic field; $\boldsymbol{g}$**:** g-tensor**;**
$\hat{\boldsymbol{S}}$**:** electron−spin operator; $\boldsymbol{D}$ **:** ZFS-tensor**;** J exchange interaction

Coupling ranges in TMI complexes		
Zeeman	≈	0 - 30 cm^{-1}
ZFS	≈	0.1- 100 cm^{-1}
HFI	≈	10^{-4} - 10^{-1} cm^{-1}
Spin-spin	≈	0 - 1000 cm^{-1}

➔ Multi-frequency EPR

Zero Field Hamiltonian

$$\hat{\mathbf{H}}_{\text{ZFS}} = \hat{\boldsymbol{S}} \cdot \mathbf{D} \cdot \hat{\boldsymbol{S}}$$

- $\boldsymbol{D}$ is diagonal in its principle axis system
- D_z has the largest absolute value
- $\boldsymbol{D}$ is traceless ($D_x + Dy + Dz = 0$).

$$\mathbf{D} = \begin{pmatrix} D_x & 0 & 0 \\ 0 & D_y & 0 \\ 0 & 0 & D_z \end{pmatrix} = \begin{pmatrix} -\frac{1}{3}D+E & 0 & 0 \\ 0 & -\frac{1}{3}D-E & 0 \\ 0 & 0 & \frac{2}{3}D \end{pmatrix}$$

$$\begin{aligned} \hat{\mathbf{H}} &= D\left(\hat{S}_z^2 - \tfrac{1}{3}S(S+1)\right) + E\left(\hat{S}_x^2 - \hat{S}_y^2\right) \\ &= D\left(\hat{S}_z^2 - \tfrac{1}{3}S(S+1)\right) + E\left(\hat{S}_+^2 + \hat{S}_-^2\right) \end{aligned}$$

$D = \dfrac{3D_z}{2}$ Axial ZFS parameter D can be positive or negative.

$E = \dfrac{D_x - Dy}{2}$ Rhombic ZFS parameter E, rhombicity $\eta = \frac{E}{D}$ with $0 \leq \eta \leq \frac{1}{3}$.

Magnetic Anisotropy

$$\hat{\mathbf{H}} = D\left(\hat{S}_z^2 - \frac{1}{3}S(S+1)\right) + E\left(\hat{S}_x^2 - \hat{S}_y^2\right)$$

- ZFS renders the magnetic properties (susceptibility) of a complex anisotropic.
  ➔ Response to an external magnetic field depends on the orientation of the molecule.
  ➔ The magnetic moment prefers to lie along a certain direction.

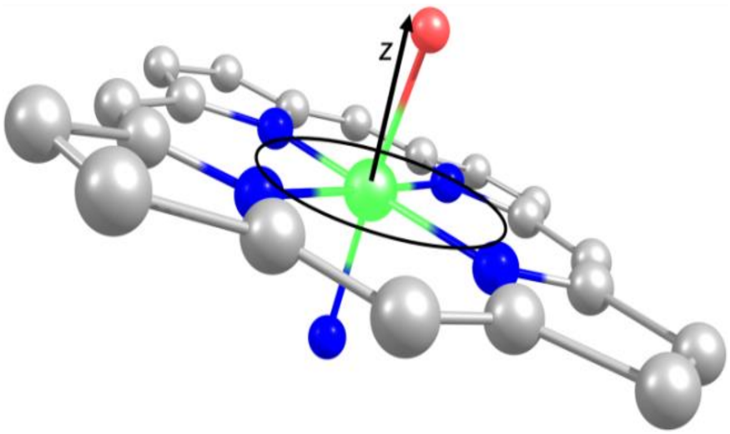

Ferric Fe porphyrin Fe^{III} ($S = 5/2$) with z-axis

- z is the main anisotropy axis.
- $D > 0$ z is "hard axis"
  Energetically most expensive to align magnetization along z.
- $D < 0$ z is "easy axis"
  Energetically cheapest to align magnetization along z.

Integer and Half Integer Spin Systems (Axial ZFS)

- Half integer spin (Kramers) and integer spin systems (Non-Kramers) have different EPR properties.
- For Non-Kramers systems, rhombic ZFS can completely lift the degeneracy of spin states.
- For Kramers systems, spin states are at least pairwise degenerate.
- D can be positive or negative, negative ZFs flips the order of the states.

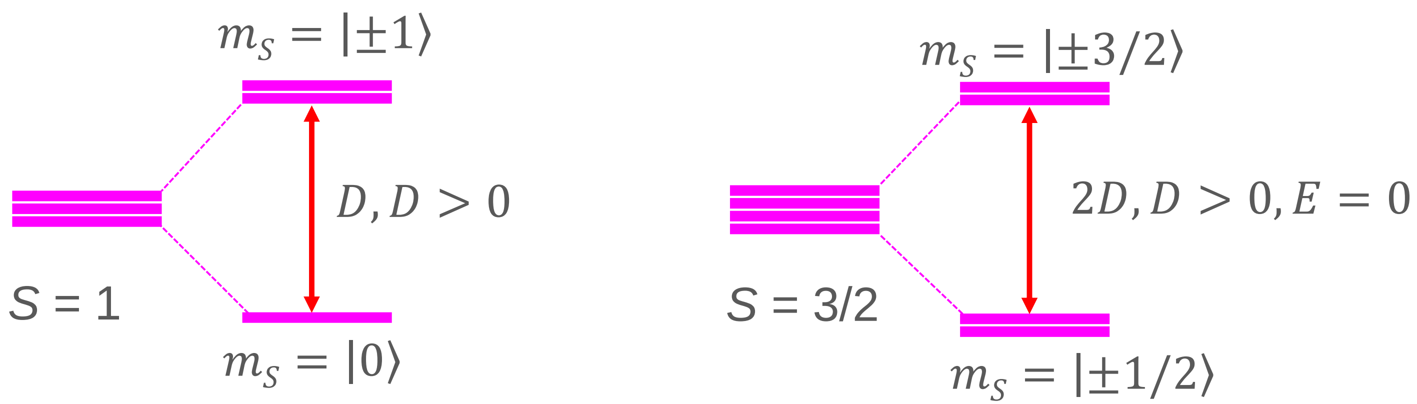

Non Kramers system

Kramers system

Integer and Half Integer Spin Systems (Rhombic ZFS)

- Half integer spin (Kramers) and integer spin systems (Non-Kramers) have different EPR properties.
- For Non-Kramers systems rhombic ZFS can completely lift the degeneracy of spin states.
- For Kramers systems spin states are at least pairwise degenerate.
- D can be positive or negative, $0 \leq \frac{E}{D} \leq \frac{1}{3}$.

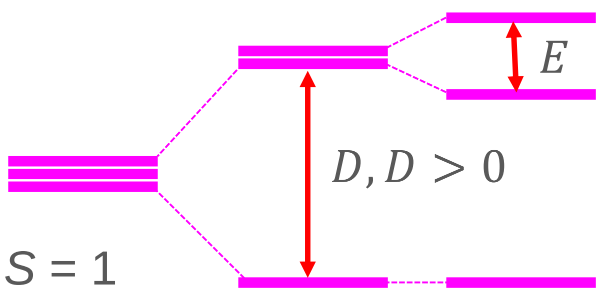

Non Kramers system

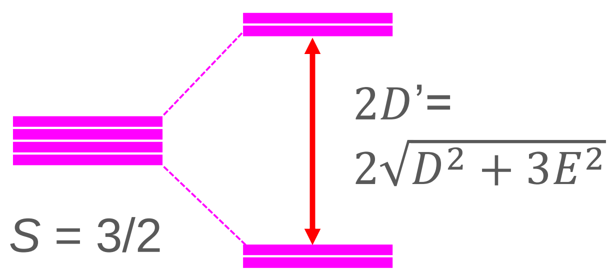

Kramers system

S > ½ Levels with ZFS

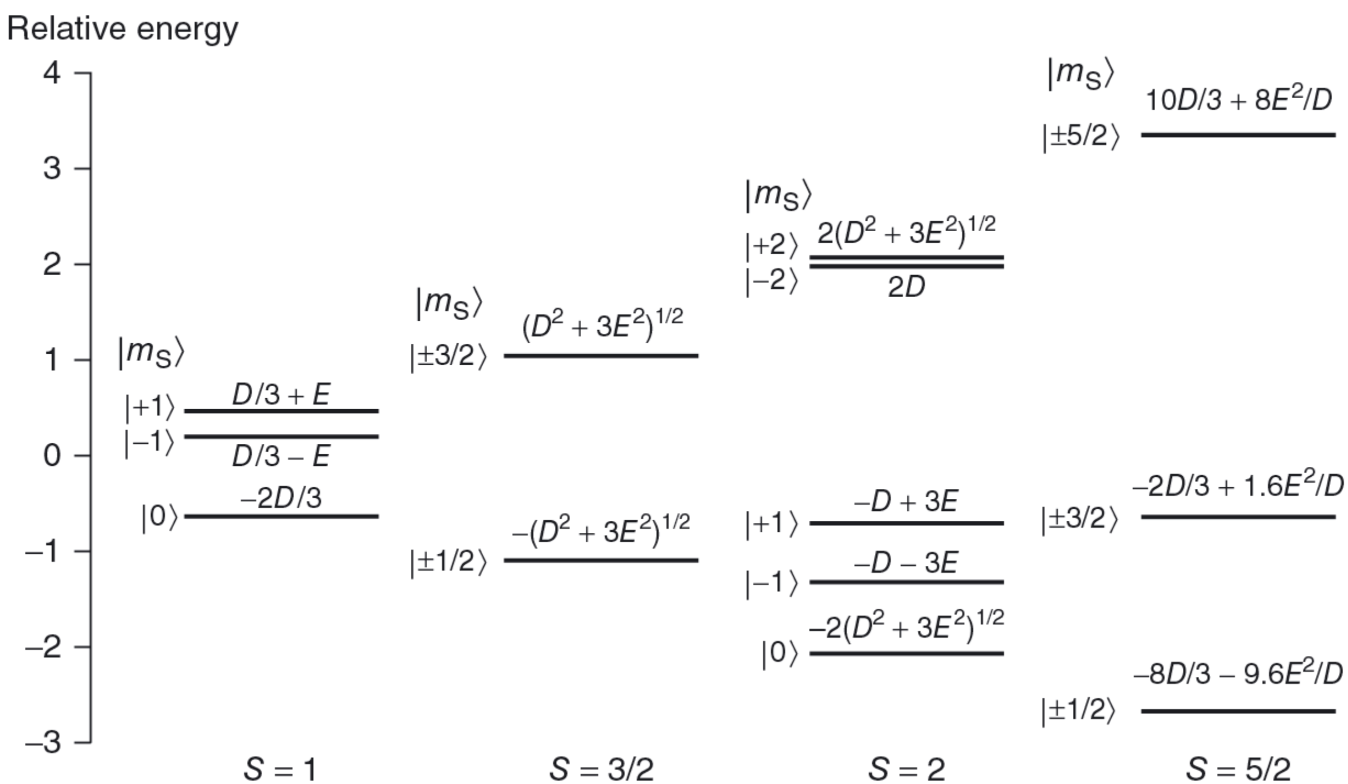

e.g. Co^{I}, Fe^{IV} | Co^{II}, Mn^{IV} | Fe^{II}, Mn^{III} | Fe^{III}, Mn^{II}

Reproduced from: Telser, J. EPR Interactions – Zero-field Splittings, ***eMagRes***; (2017) 207

Note: E lifts degeneracy of $2S+1$ integer-spin levels (Non Kramers system)
E shifts half-integer spin levels (Kramers system)
For $E > 0$ m_S is not a good quantum number at low field.

Weak Magnetic Field Regime: S = 1 (Non-Kramers System)

$D \gg g\mu_B B$

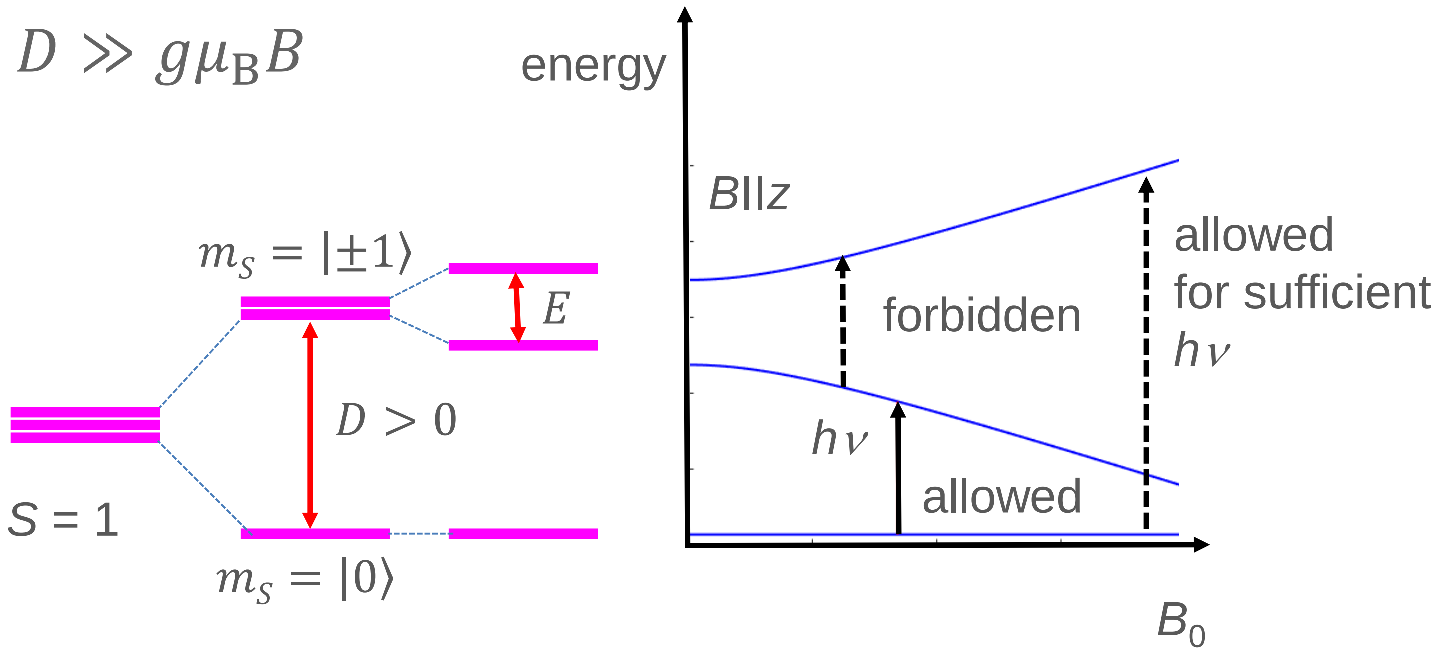

Non-Kramers systems are often „EPR silent“ in the weak field regime. Typical examples Fe^{IV} , Mn^{III} (S =1 and S =2) Fe^{II} (S = 2) and Co^{I} (S =1). Can exhibit $D \gg$ 3 cm^{-1} (~ 100 GHz), which renders them EPR silent at X, Q, and W-band.

Strong Field Regime: $S = 1$ (Non-Kramers System)

$D \ll g\mu_B B$

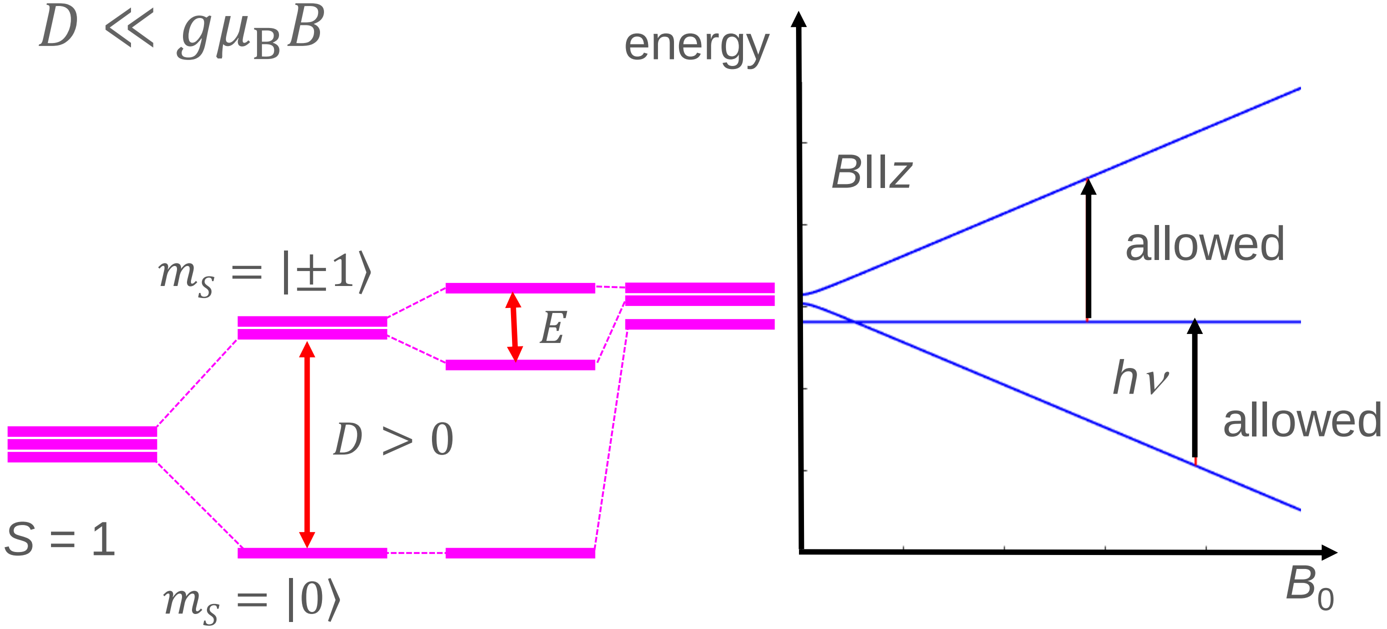

S = 1 give rise to triplet spectra in the strong field regime.
Typical examples are organic triplets see talk by Serge Gambarelli

Strong Field Regime Orientation Dependent Triplet Levels

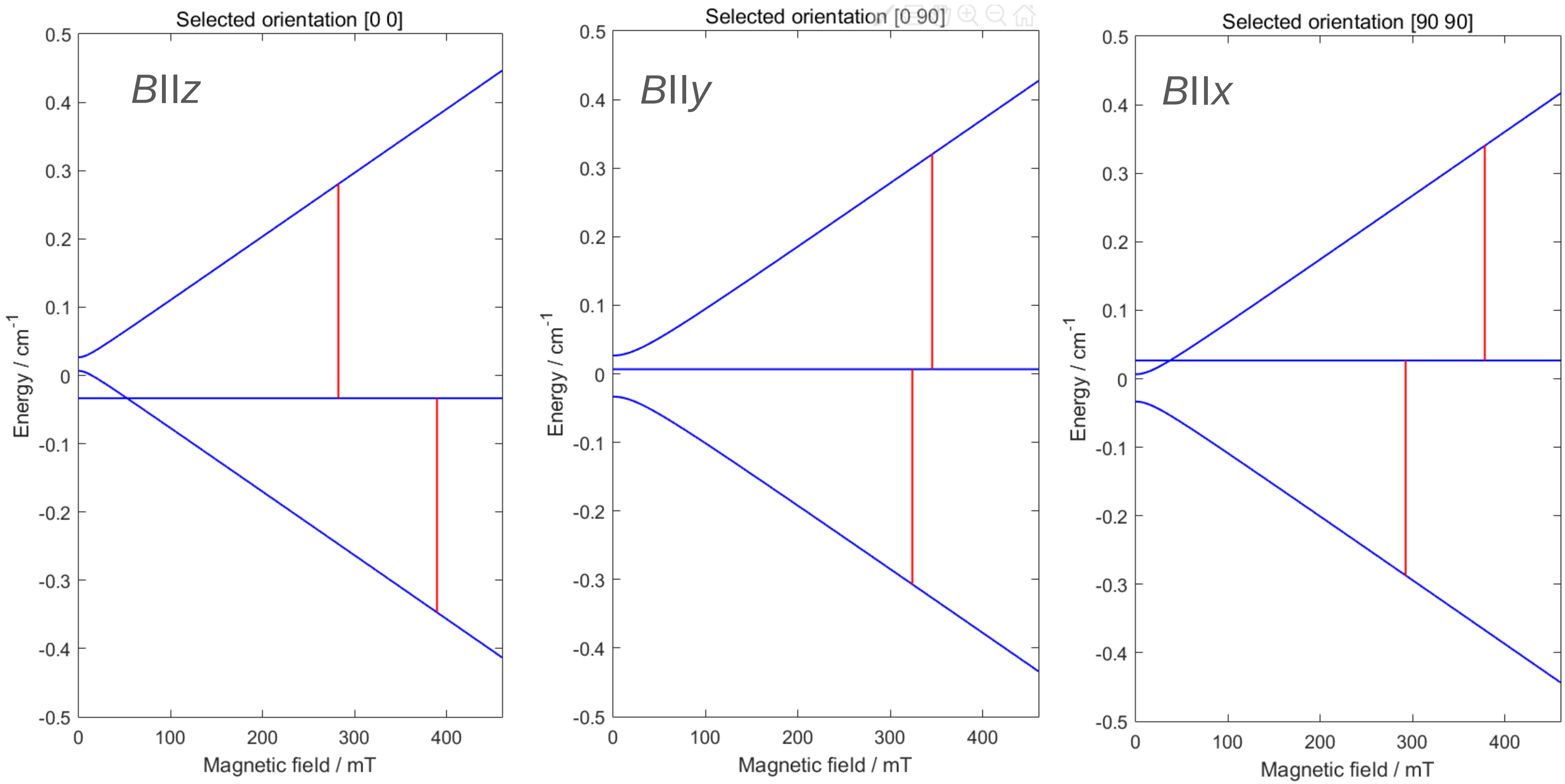

$S = 1,\ D > 0, E = \frac{1}{5}D$

x, y and z are molecular axes

Strong Field Regime: Triplet Powder Spectrum

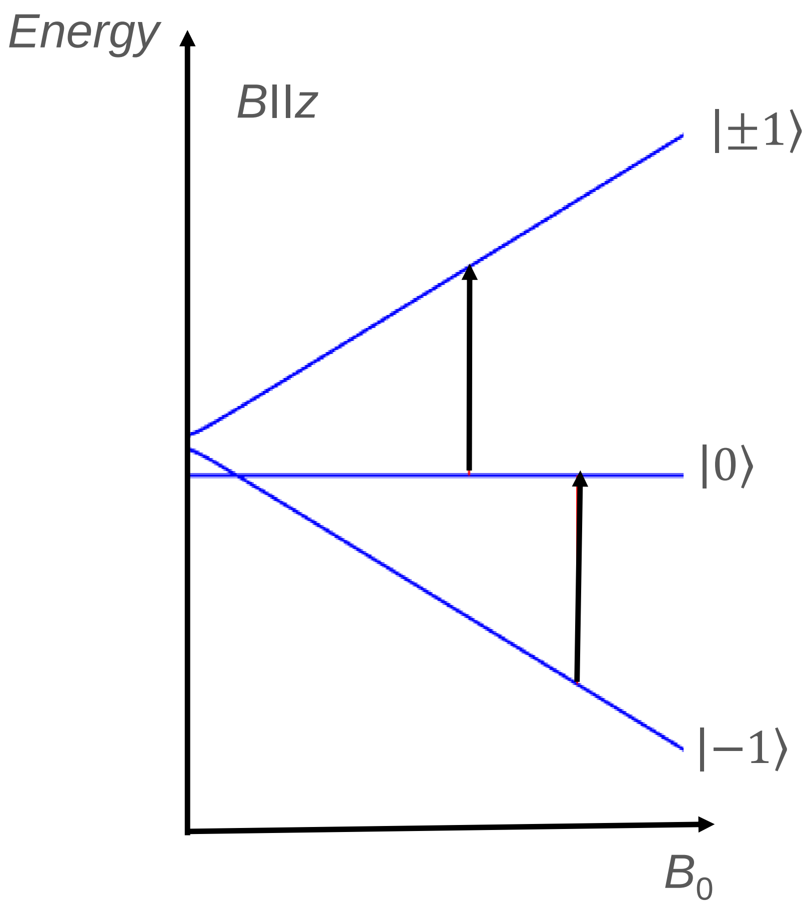

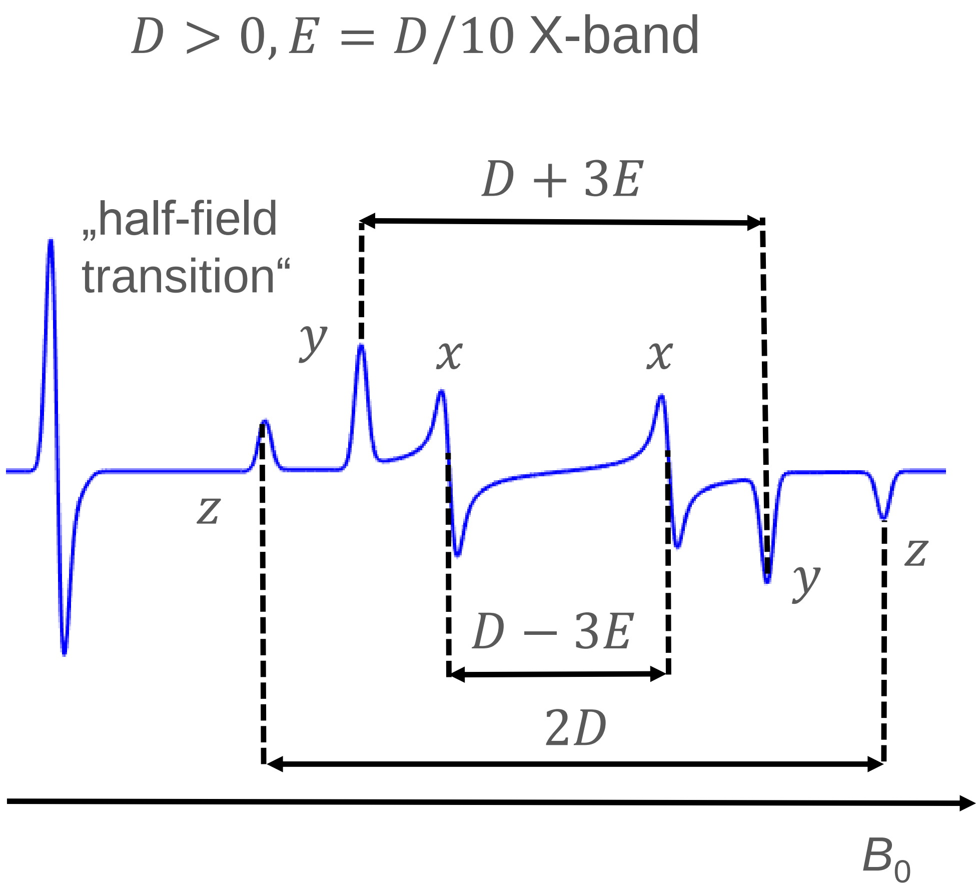

See talks by Serge Gambarelli, and Stefan Stoll

Example: W-band EPR of the S_3 ($S = 3$) State in PSII

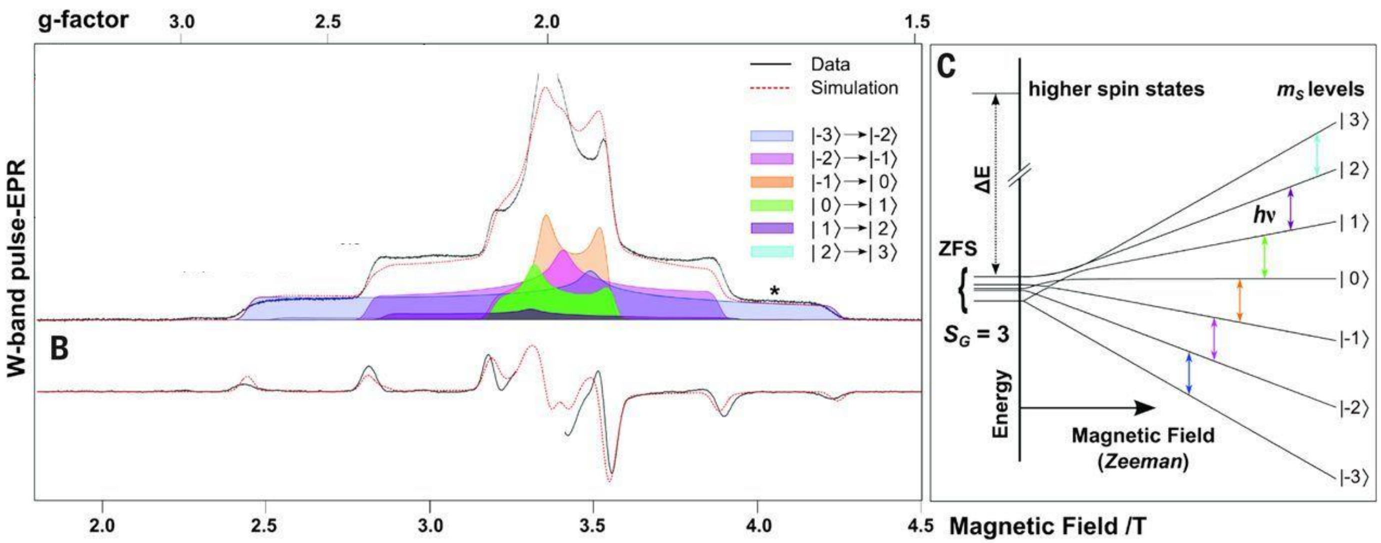

Four $\mathrm{Mn^{IV}}$ ($S = 3/2$)
couple to $S = 3$
D/hc = −0.175 cm^{-1}

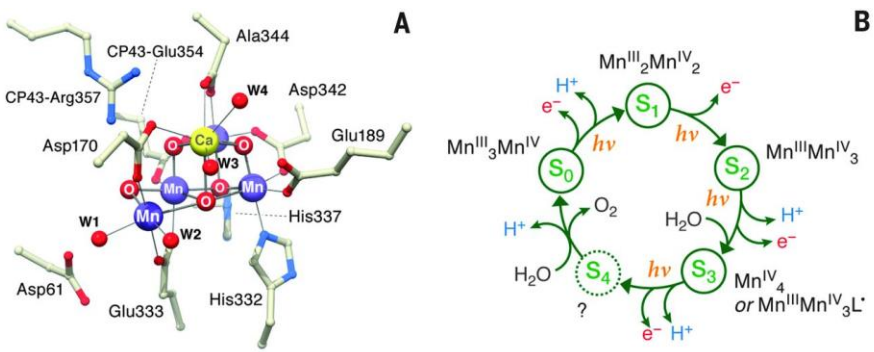

N. Cox, et al. ***Science*** 345, 804 (2014)
Bouusac et al. ***JACS*** 131(14), 15 (2009)

Summary Non-Kramers High Spin States

- Non-axial ZFS lifts the degeneracy of Non-Kramers states.
- For large D, microwave quanta and external magnetic fields available in conventional EPR spectrometers (10 GHz/0.3 cm^{-1} for X-band vs. D/hc = 1-100 cm^{-1}) are often not sufficient to excite EPR transitions.
- No easily observable $m_S = \pm {}^1/_2$ transitions
- Integer high-spin systems are often “EPR silent”

➔ EPR detection requires high-frequencies.

- Mixing of Non-Kramers pairs (by rhombic ZFS) gives rise to EPR transitions with the microwave magnetic field component polarized parallel to the external magnetic field.

➔ May be detected by parallel mode EPR

See poster of Alvaro Montoya

Weak Field Regime: $S = 3/2$ (Kramers System); Axial ZFS

$D \gg g\mu_B B$

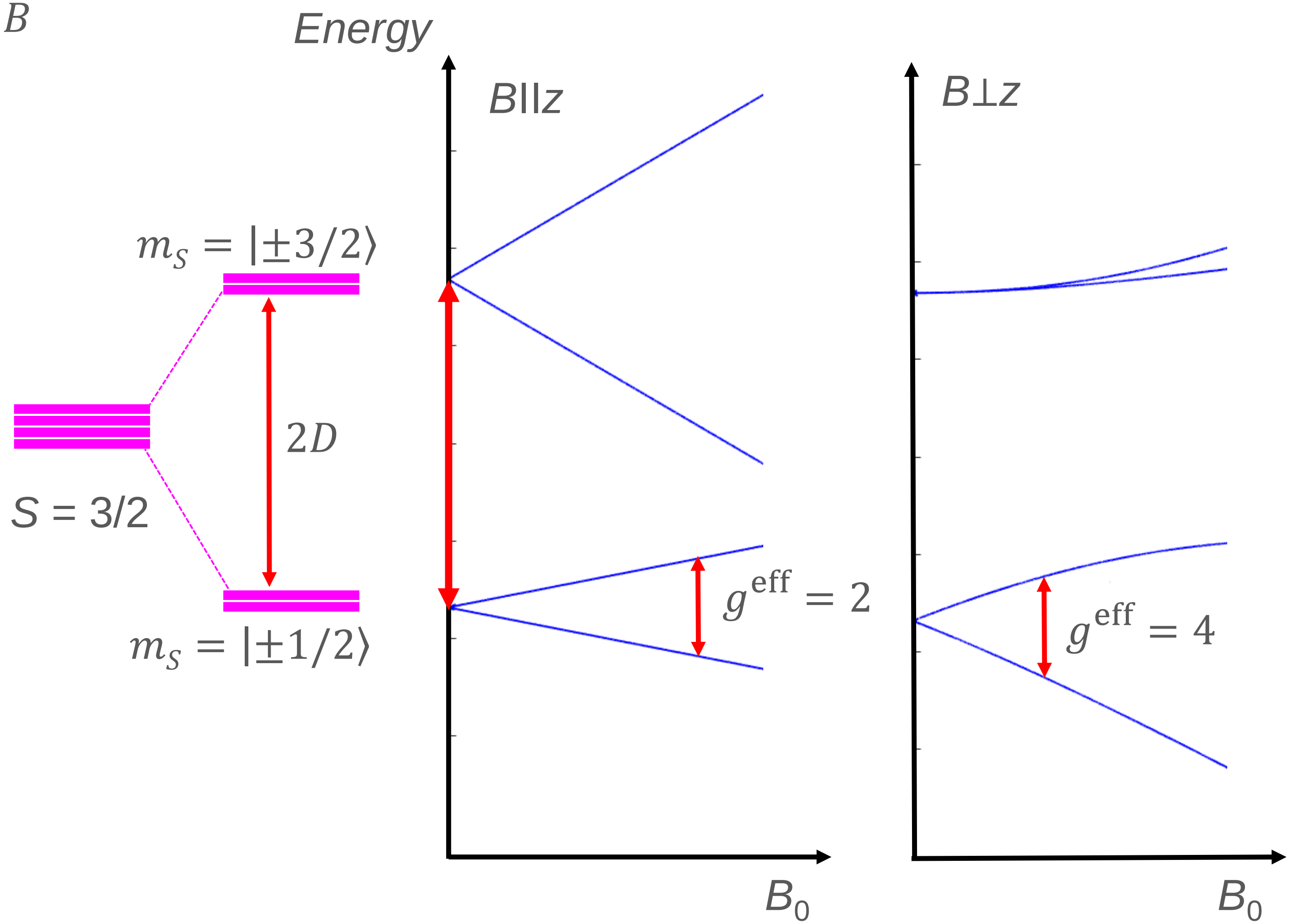

$S = 3/2\,, D > 0, E = 0;$

Weak Field Regime: $S = 5/2$ (Kramers System), Axial ZFS

$D > 0, E = 0$

➔ EPR from $|\pm 1/2\rangle$ transitions, intensity decreases with temperature.

$D < 0, E = 0$

➔ EPR from $|\pm 1/2\rangle$ transitions, intensity increases with temperature.

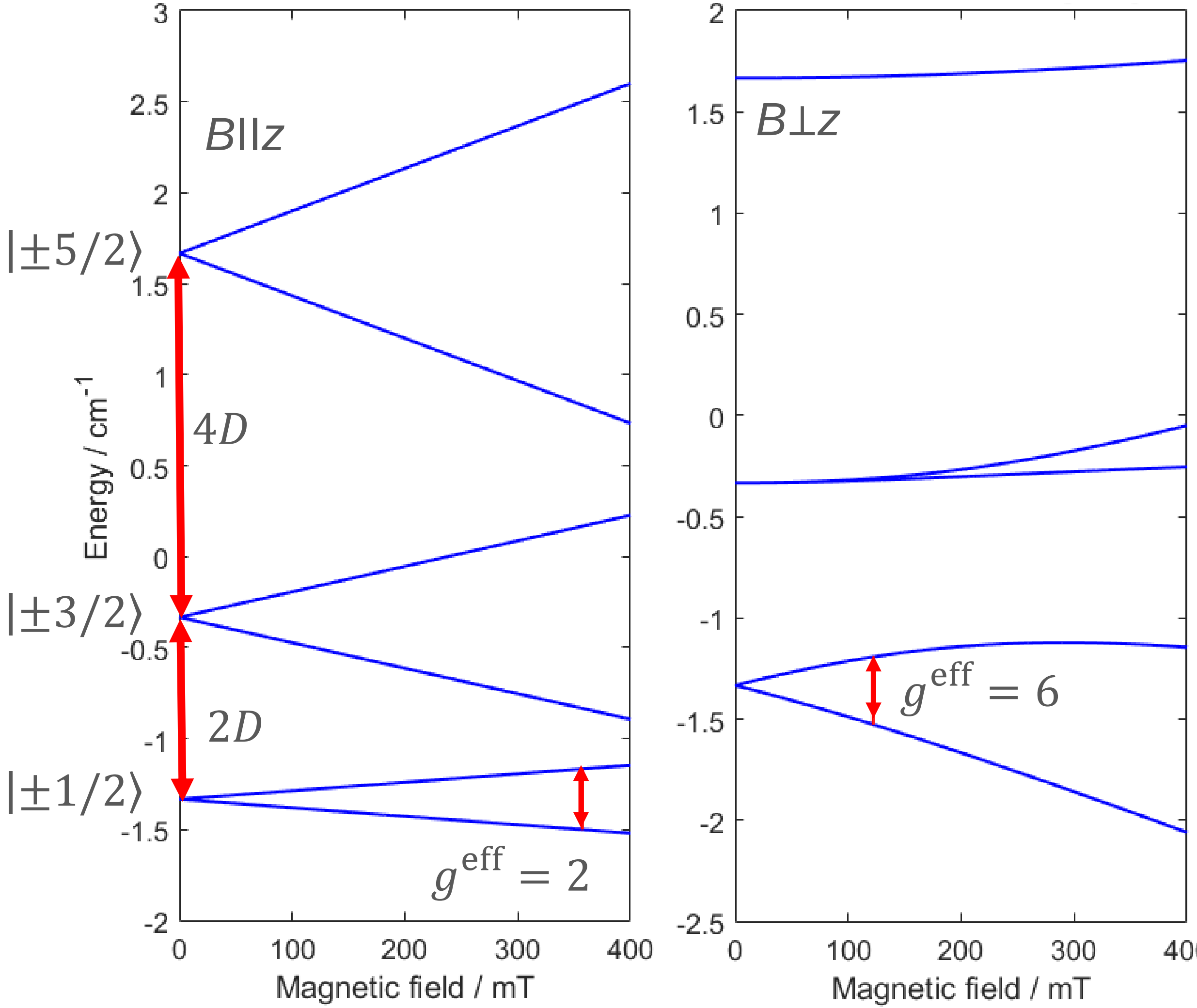

$S = 5/2, D > 0, E = 0;$

Mn^{II} ($S = 5/2, I = 5/2$) Strong Field to Weak Field Regime

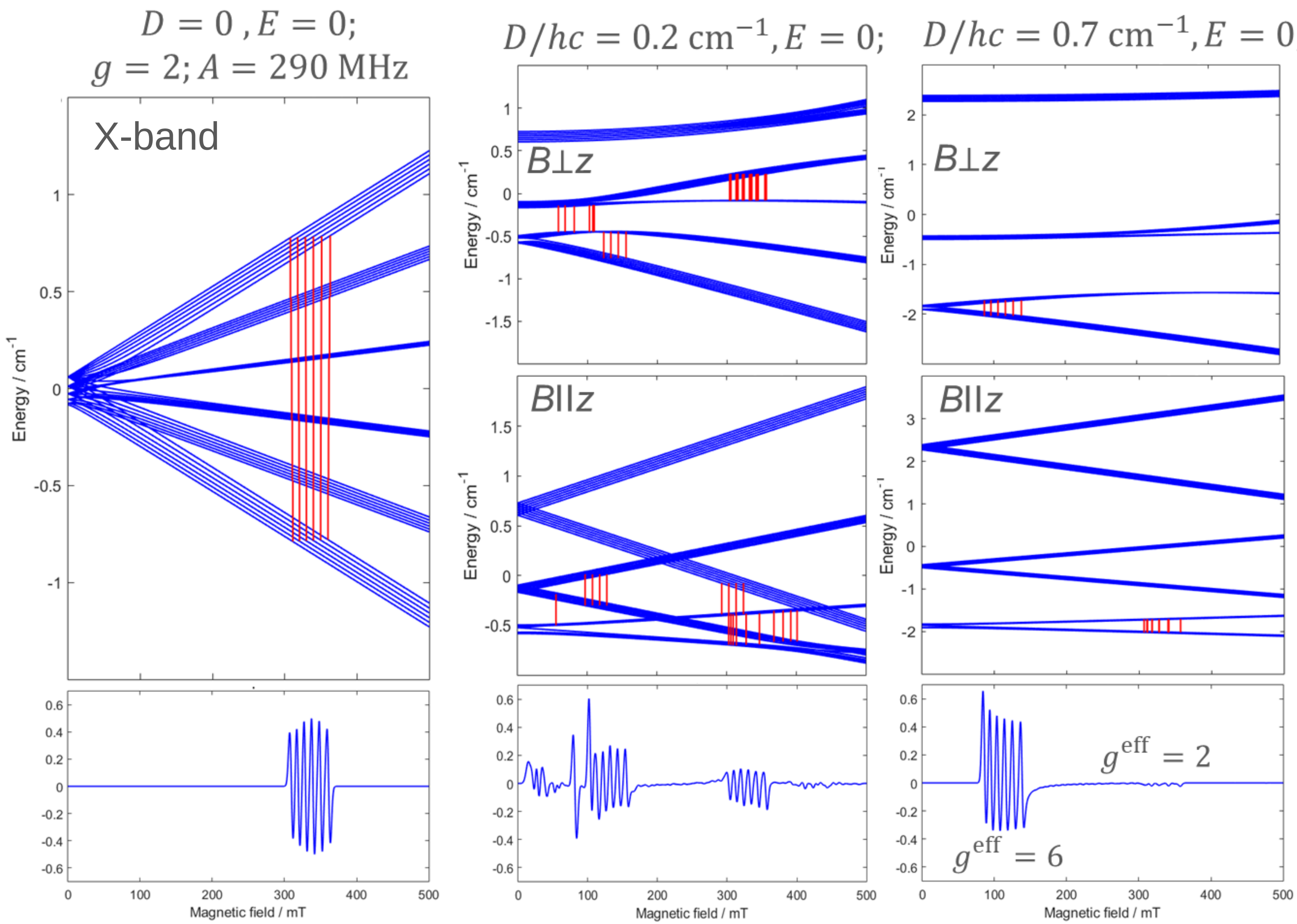

Weak Field Regime: $S = 5/2$ effective g-values

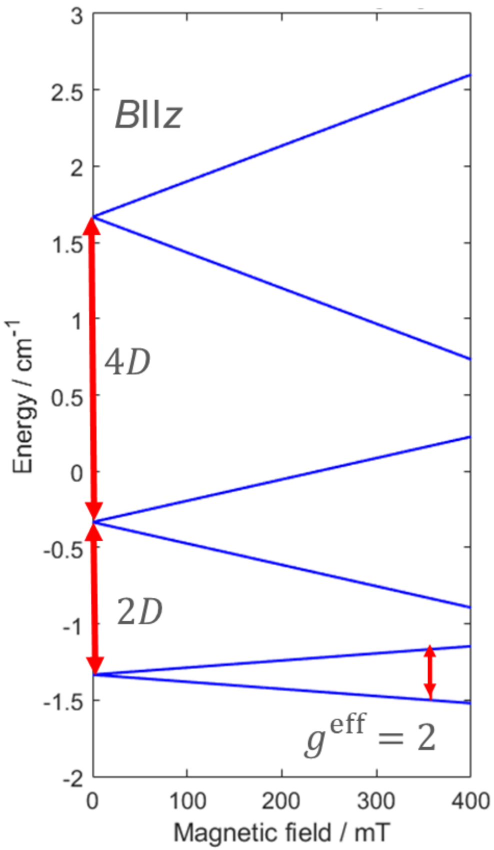

See example *Fundamental Theory problem 5*
Pilbrow, ***JMR*** 31,479 (1978),
Hagen, ***Dalton Trans.*** 37 4415 (2006

$D \gg g\mu_B B$ Kramers systems can be described by $S^{\mathrm{eff}} = \frac{1}{2}$.

$$\hat{\mathrm{H}} = \mu_{\mathrm{B}} \boldsymbol{B}_0 \mathbf{g}^{\mathrm{eff}} \boldsymbol{S}^{\mathrm{eff}}$$

and g^{eff} for each Kramers doublet, e.g. for $S = 5/2$ in near axial symmetry ($E \ll D$) for $|\pm 1/2\rangle$ transitions :

$$g_x^{\mathrm{eff}} = 3g_x \left[1 - \frac{(g_y \mu_{\mathrm{B}} B)^2}{2D^2} - \left(\frac{4E}{D}\right)\right]$$

$$g_y^{\mathrm{eff}} = 3g_y \left[1 - \frac{(g_y \mu_{\mathrm{B}} B)^2}{2D^2} + \left(\frac{4E}{D}\right)\right]$$

$$g_z^{\mathrm{eff}} \approx 2$$

For $g_x \approx g_y \approx g_z \approx 2$. (e.g. in Fe^{III})

$$g_{\parallel}^{\mathrm{eff}} \approx 6 \pm 24E/D$$

$$g_{\perp}^{\mathrm{eff}} \approx 2$$

EPR transitions depend solely on E/D.

g^{eff} can be plotted in rhombogram for each transition.

Weak Field Regime: $S = 5/2$ Rhombograms

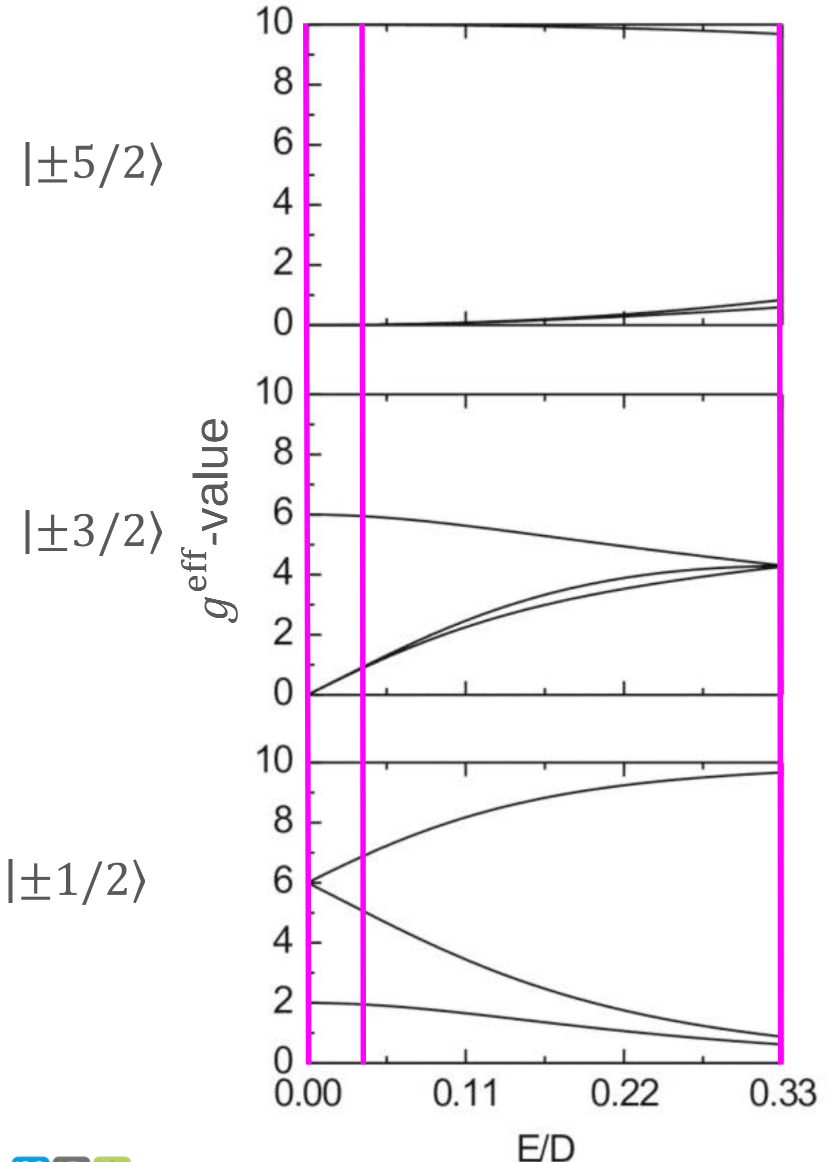

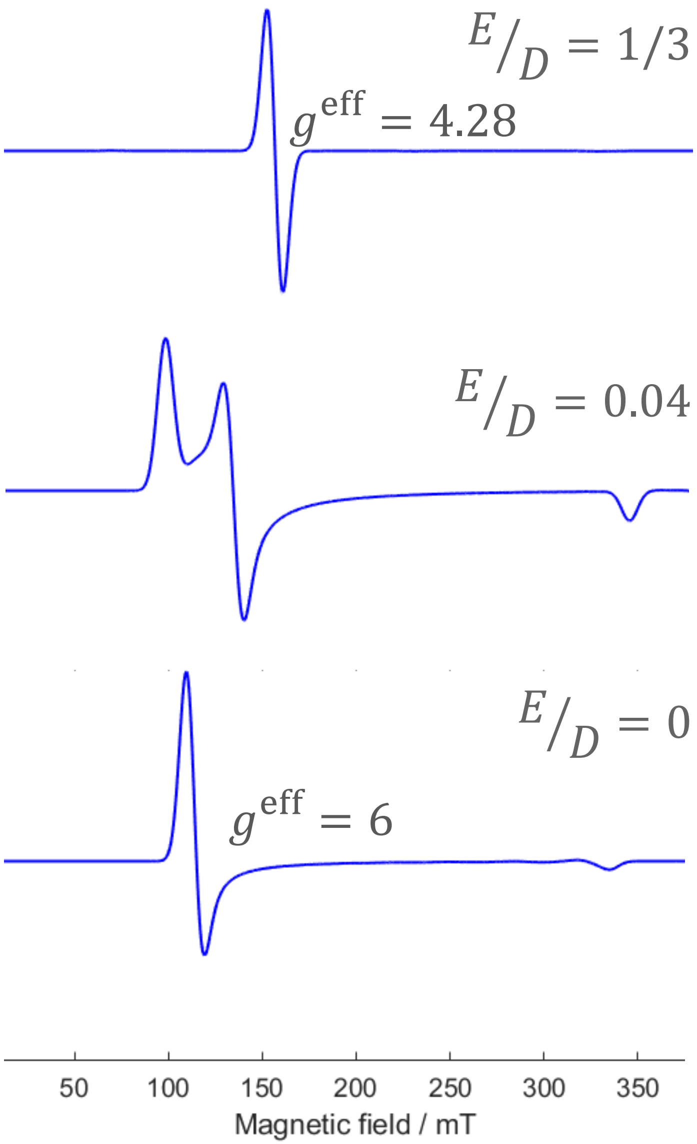

Weak Field Regime: $S = 5/2$ Rhombograms

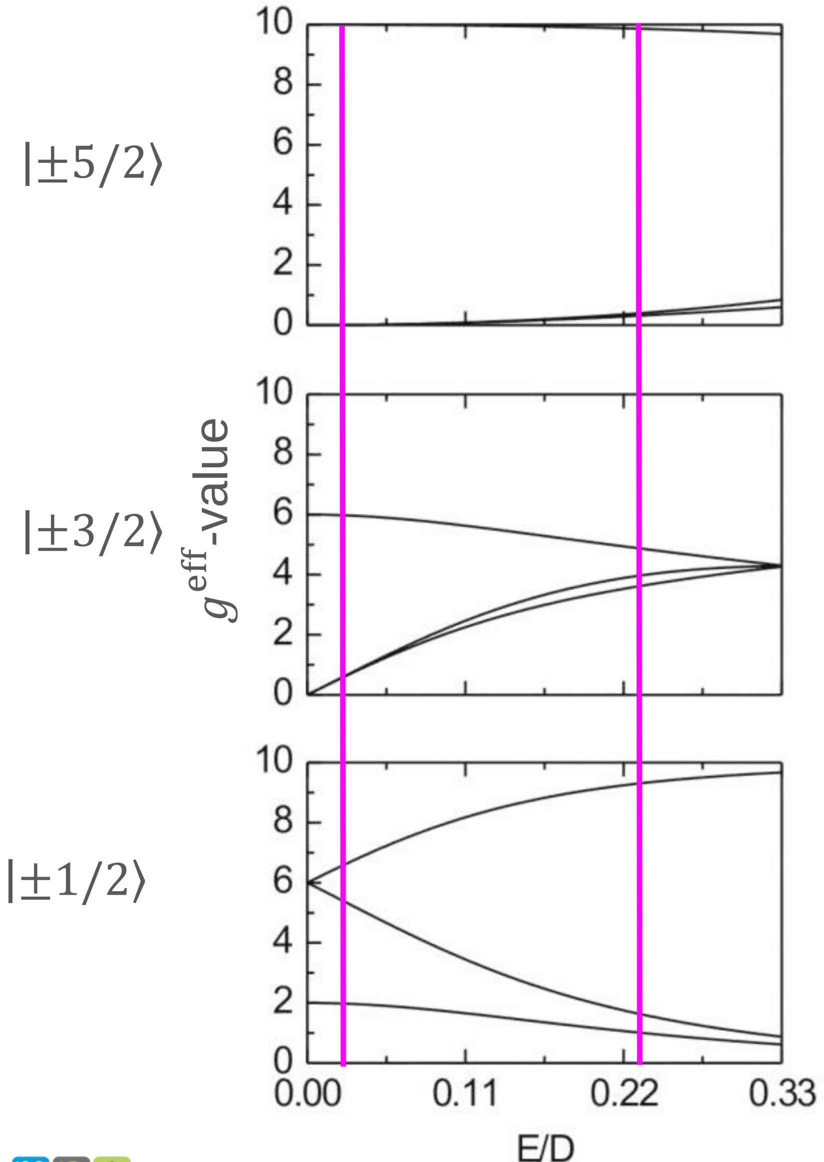

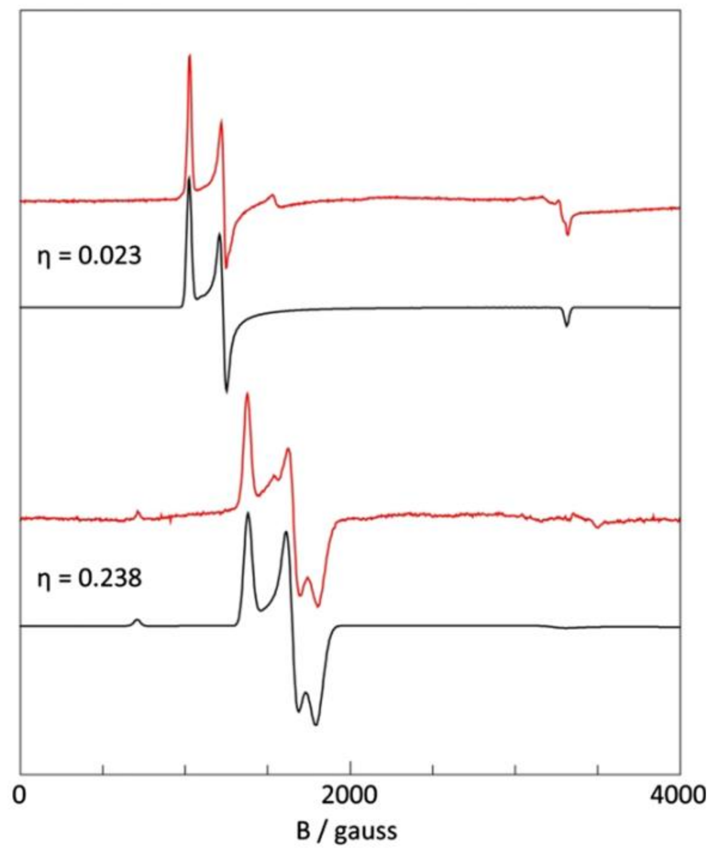

X-band Cw EPR of Fe^{III} (S =5/2) in *Penicillium simplicissimum* catalase (top) and in *Escherichia coli* iron superoxide dismutase.

Hagen, Practical Approaches to Biological Inorganic Chemistry, Chap. 3, Elsevier, 2013
see poster: Ilenia Serra

Summary Kramers $S > ½$ States

- For Kramers systems spin states are at least pairwise degenerate.
- $m_S = \pm {}^1/_2$ transitions observable in most cases (exception $D < 0, E = 0$ at low temperature).
- In the weak field regime conventional EPR provides information on spin states and ${}^E/_D$
- The temperature dependence of X-band EPR reveals sign of D.
- For large ZFS, precise determination of $|D|$ requires high-frequency EPR.

Half Integer and Integer Spin Energy Levels

$$\hat{H} = D(\hat{S}_z^2 - {}^1/_3\, S(S+1)) + \mu_B \boldsymbol{B}_0 \cdot \boldsymbol{g} \cdot \hat{\boldsymbol{S}}$$

$S = 3/2$ $D/hc = 24.4$ cm^{-1}

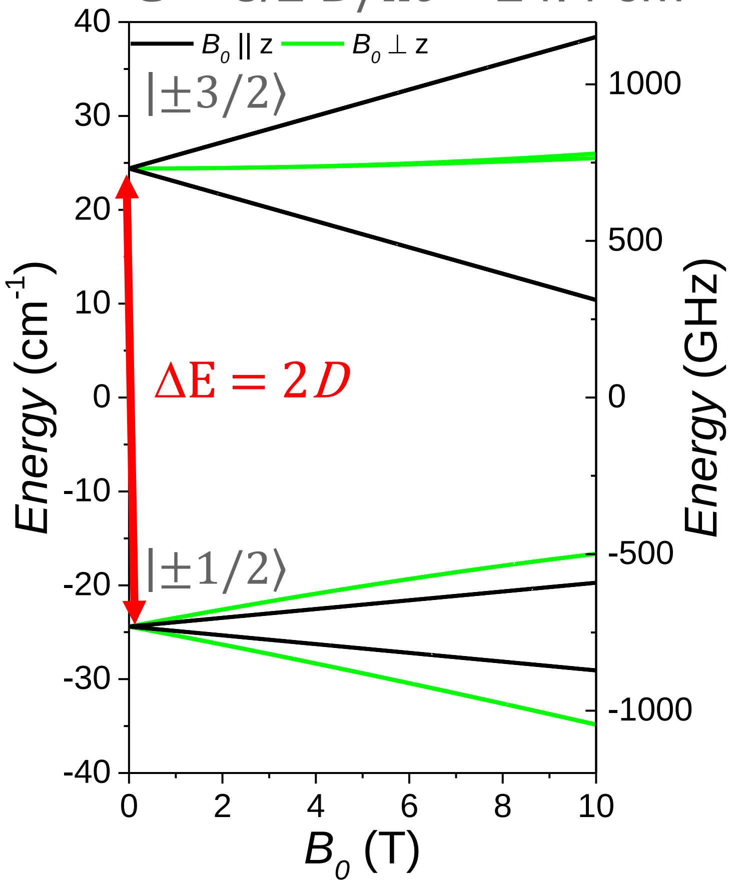

$S = 1$ $D/hc = 16.4$ cm^{-1}

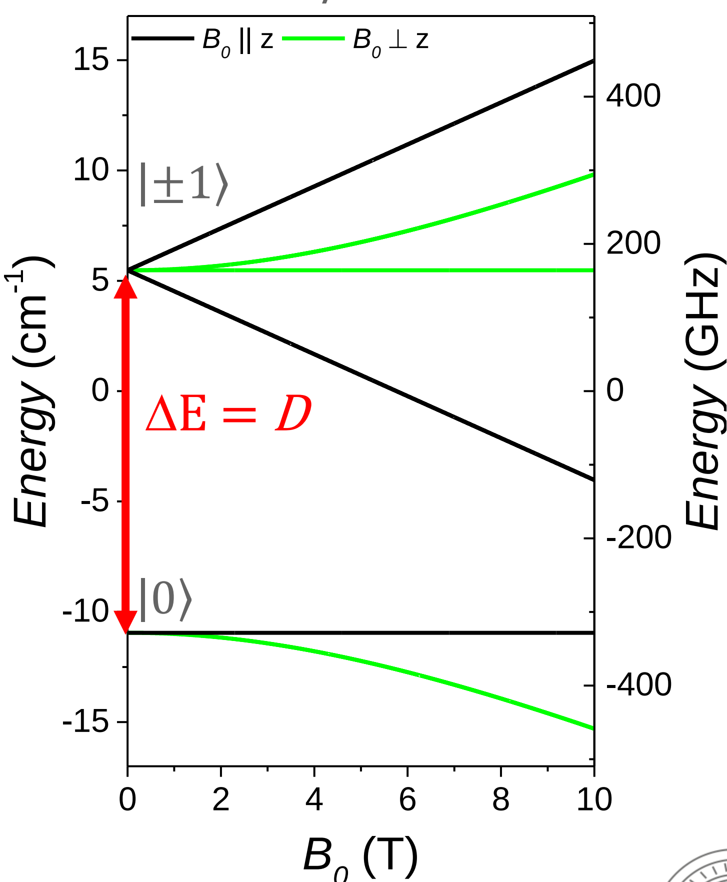

Normalization to Ground States

$$\hat{H} = D(\hat{S}_z^2 - {}^1/_3\, S(S+1)) + \mu_B \boldsymbol{B}_0 \cdot \boldsymbol{g} \cdot \hat{\boldsymbol{S}}$$

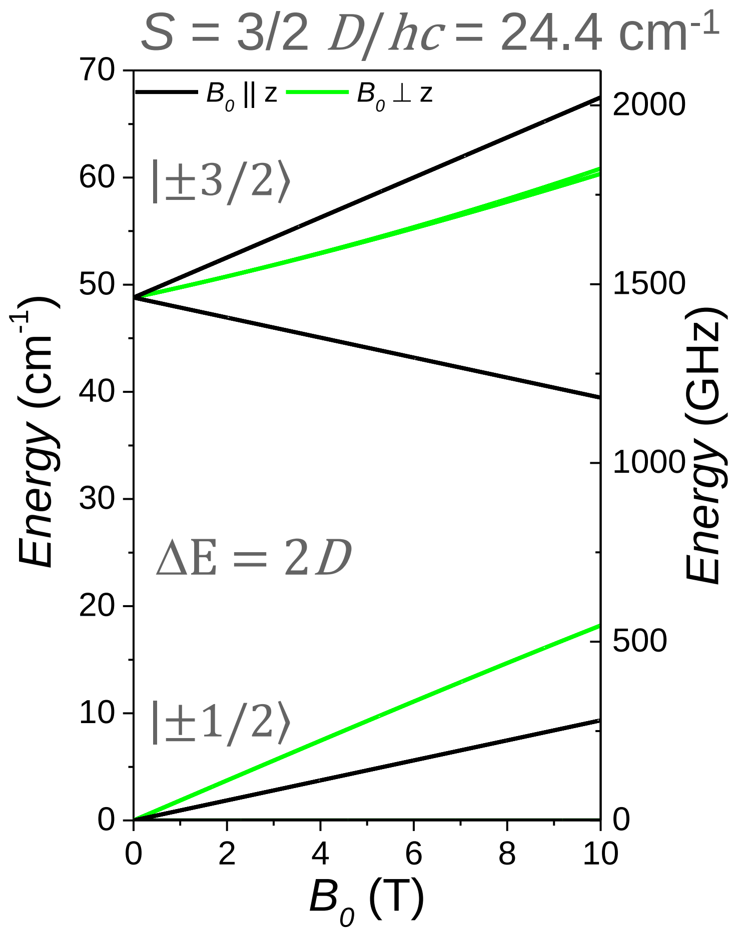

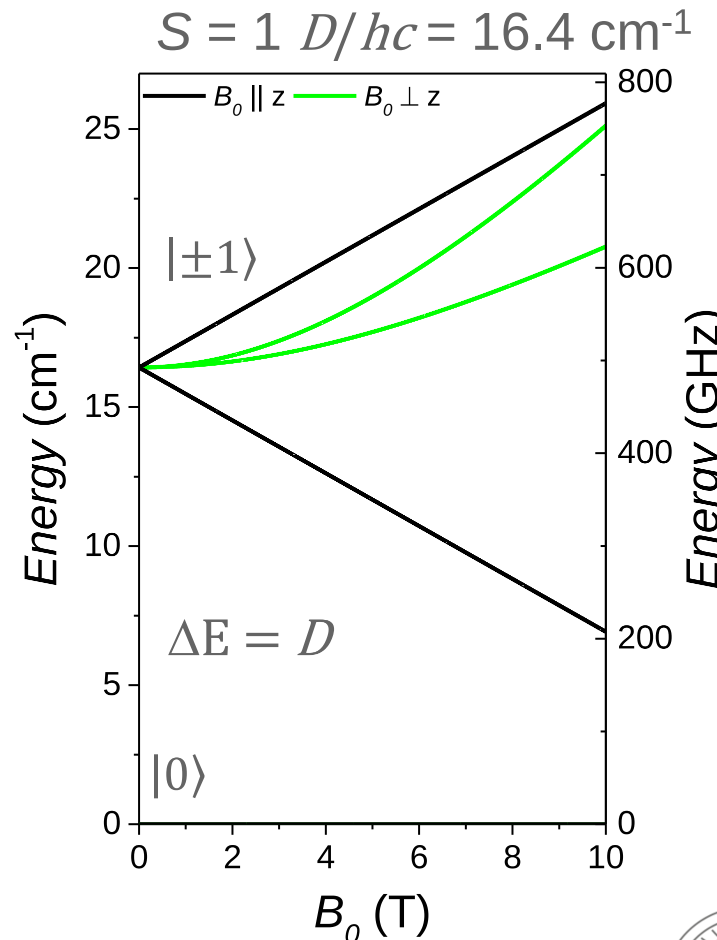

Field vs. Frequency Domain EPR (S = 1)

S = 1
g = 2
D/h = 535 GHz,
D/hc = 17.85 cm^{-1}
E/h = 12.5 GHz,
E/hc = 0.42 cm^{-1}

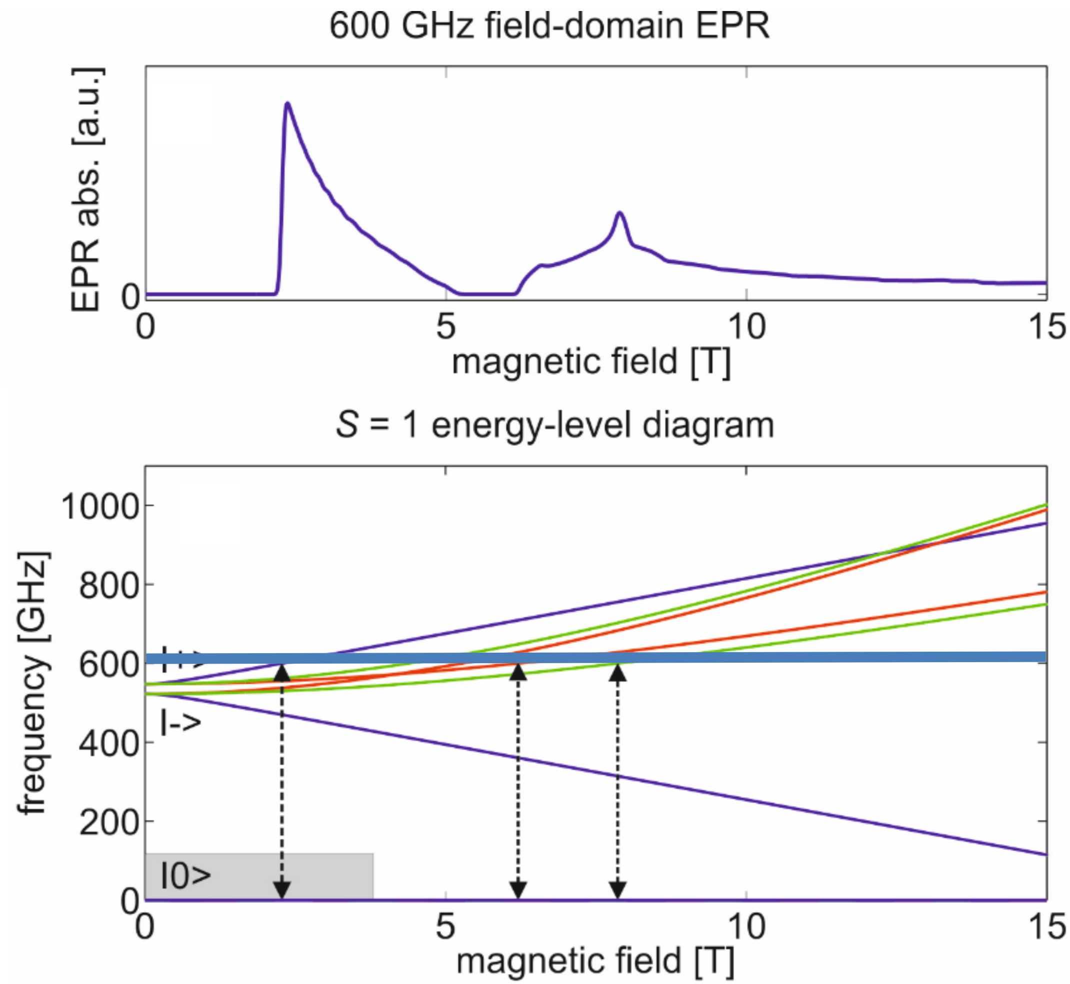

Schnegg, A., ***eMagRes***, *6*, (2017) 115.

green: B_0||x, red: B_0||y and blue: B_0||z

Field vs. Frequency Domain EPR (S = 1)

S = 1
g = 2
D/h = 535 GHz,
D/hc = 17.85 cm^{-1}
E/h = 12.5 GHz,
E/hc = 0.42 cm^{-1}

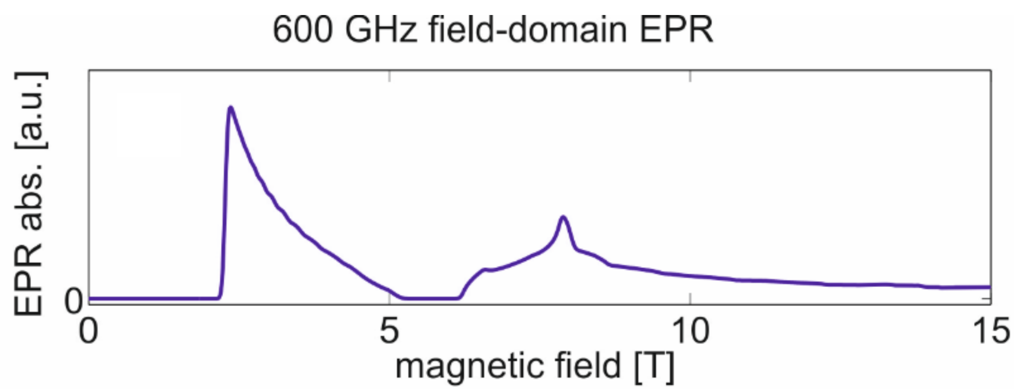

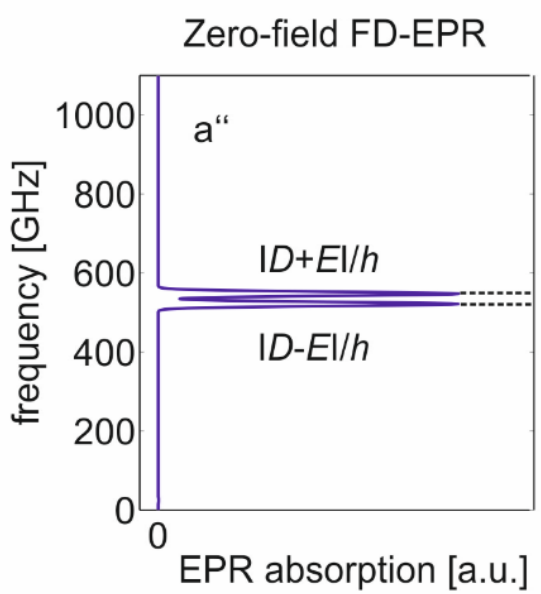

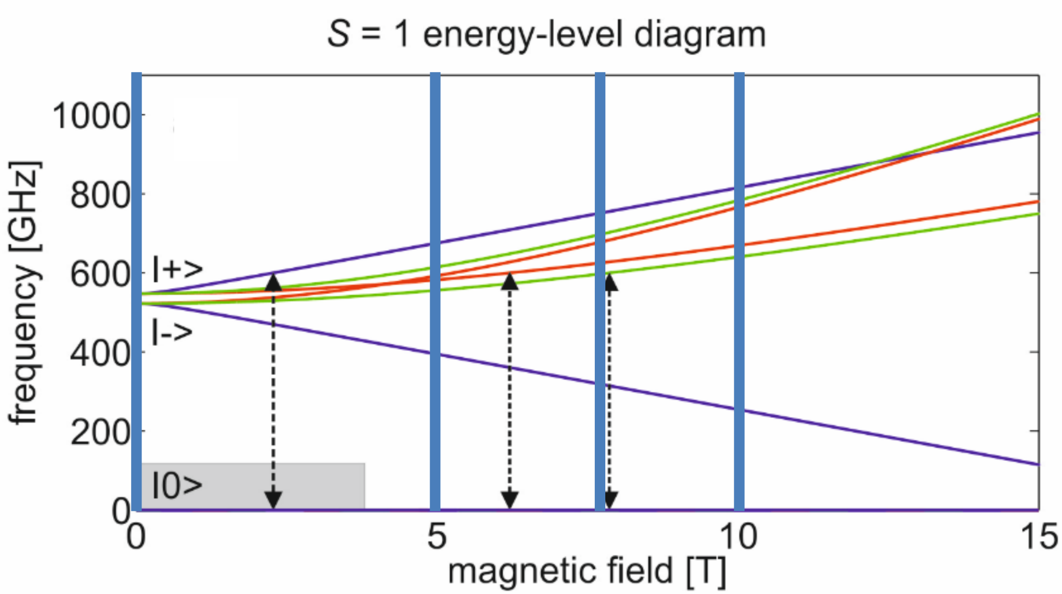

Schnegg, A., ***eMagRes***, *6*, (2017) 115.

green: B_0||x, red: B_0||y and blue: B_0||z

Field vs. Frequency Domain EPR (S = 3/2)

$S = 1$
$g = 2$
D/h = 535 GHz,
D/hc = 17.85 cm^{-1}
E/h = 12.5 GHz,
E/hc = 0.42 cm^{-1}

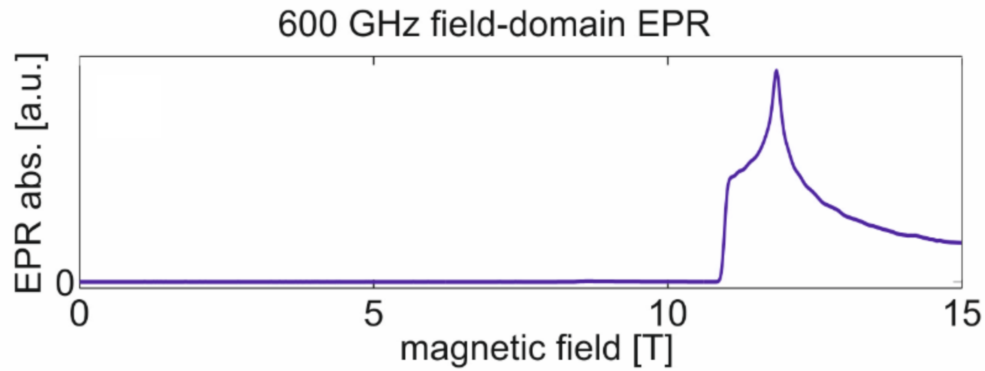

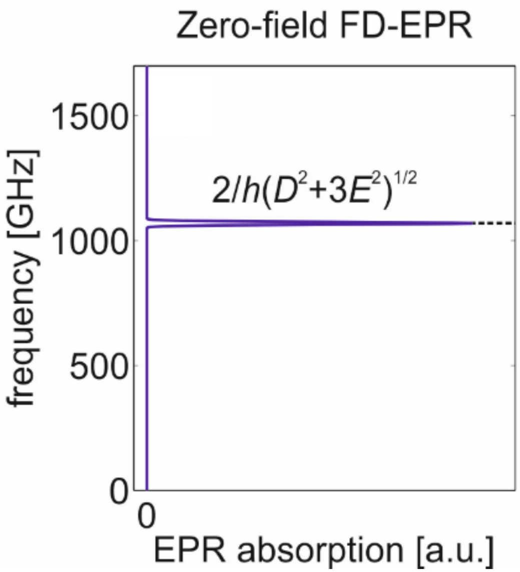

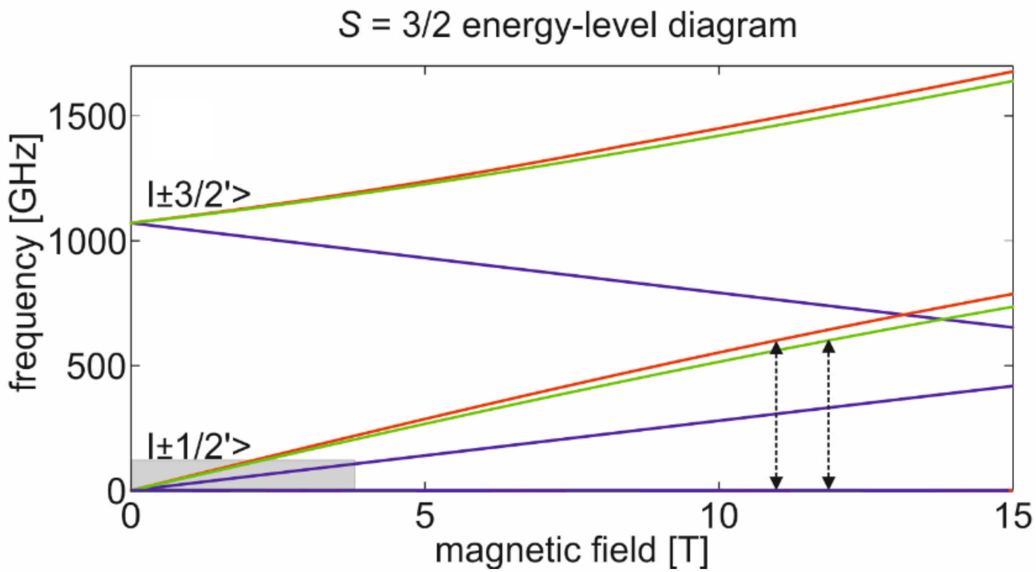

Schnegg, A., ***eMagRes***, *6*, (2017) 115.

green: B_0||x, red: B_0||y and blue: B_0||z

Broad-band EPR Detection Techniques

Method	Advantages/Disadvantages	Available e.g.
Single- or multi-high frequency EPR *Fixed frequency - swept field*	+ Pulsed/CW modes + High resolution + High sensitivity (resonators) – Multi frequency requires several sources/spectrometers	FZ Rossendorf, NHMFL Tallahassee LNCMI Grenoble
Frequency Domain Magnetic Resonance (FDMR) *Fixed field - swept frequency*	+ EPR at zero magnetic field + High resolution – Broad scans require several sources	Uni Stuttgart IFW Dresden Brno
FD-FT THz-EPR *Fixed field - swept frequency*	+ EPR at zero magnetic field + Only one source necessary + Very broad excitation frequency range – Limited resolution	HZB (Synchrotron) Uni Stuttgart FZ Rossendorf
THz-Time Domain Spectroscopy (THz-TDS spectroscopy) *Fixed field - swept frequency*	+ EPR at zero magnetic field + High excitation power + Only one source necessary – Limited resolution	MIT

Multifrequency „Florida plot“ of Co^{II} $S = 3/2$

627 GHz EPR

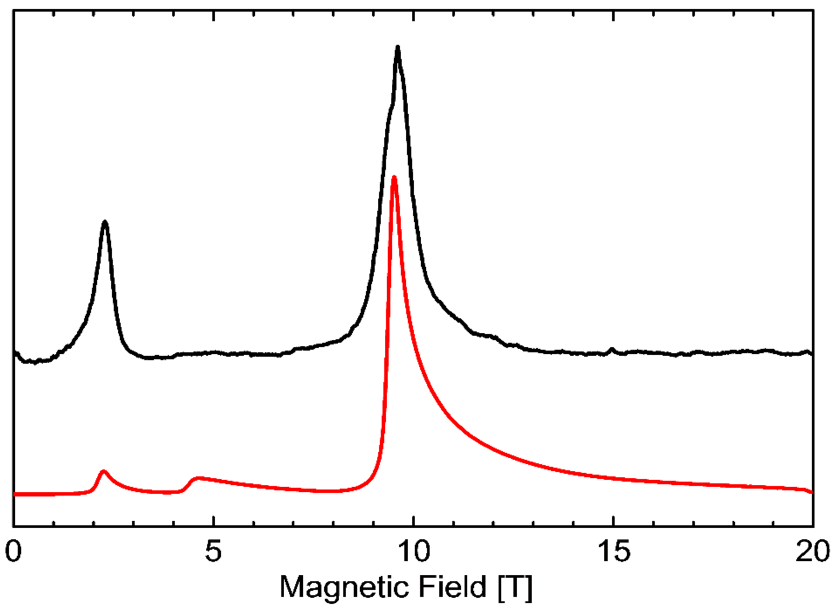

Transition frequency-field plot

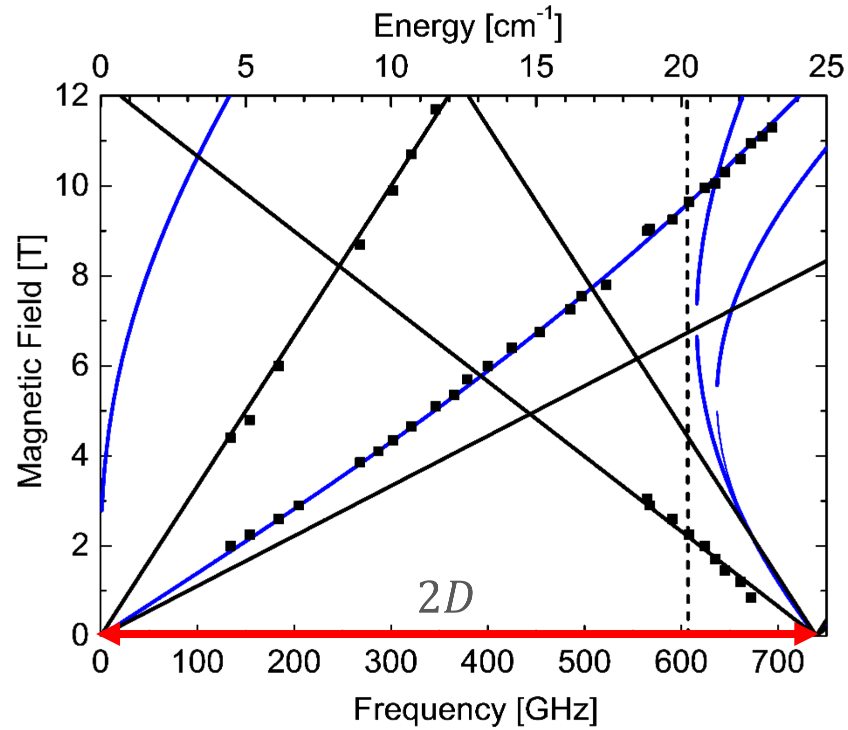

Tp^{Np,H}Co(NCO) (Tp^{NP,H} = hydro(3-Np,5-H-trispyrazolyl)borate anion; Np = neopentyl) at 4.2 K.

Co^{II}, $S = 3/2$, D/hc = +12.32(5) cm^{-1},E/hc = 0.07(9) cm^{-1},

$g\perp$ = 2.54(3), $g||$ = 2.14(2))

Reproduced after Telser, Electron Paramagnetic Resonance: Vo. 23, Ch. 22 (2013)

FD-FT THZ-EPR

Energy range:
3 cm^{-1} – 600 cm^{-1}
Magnetic field:
+11 T to -11 T
Temperature:
1.5 K to RT

FD-FT THZ-EPR
@ BESSY II, HZB Berlin

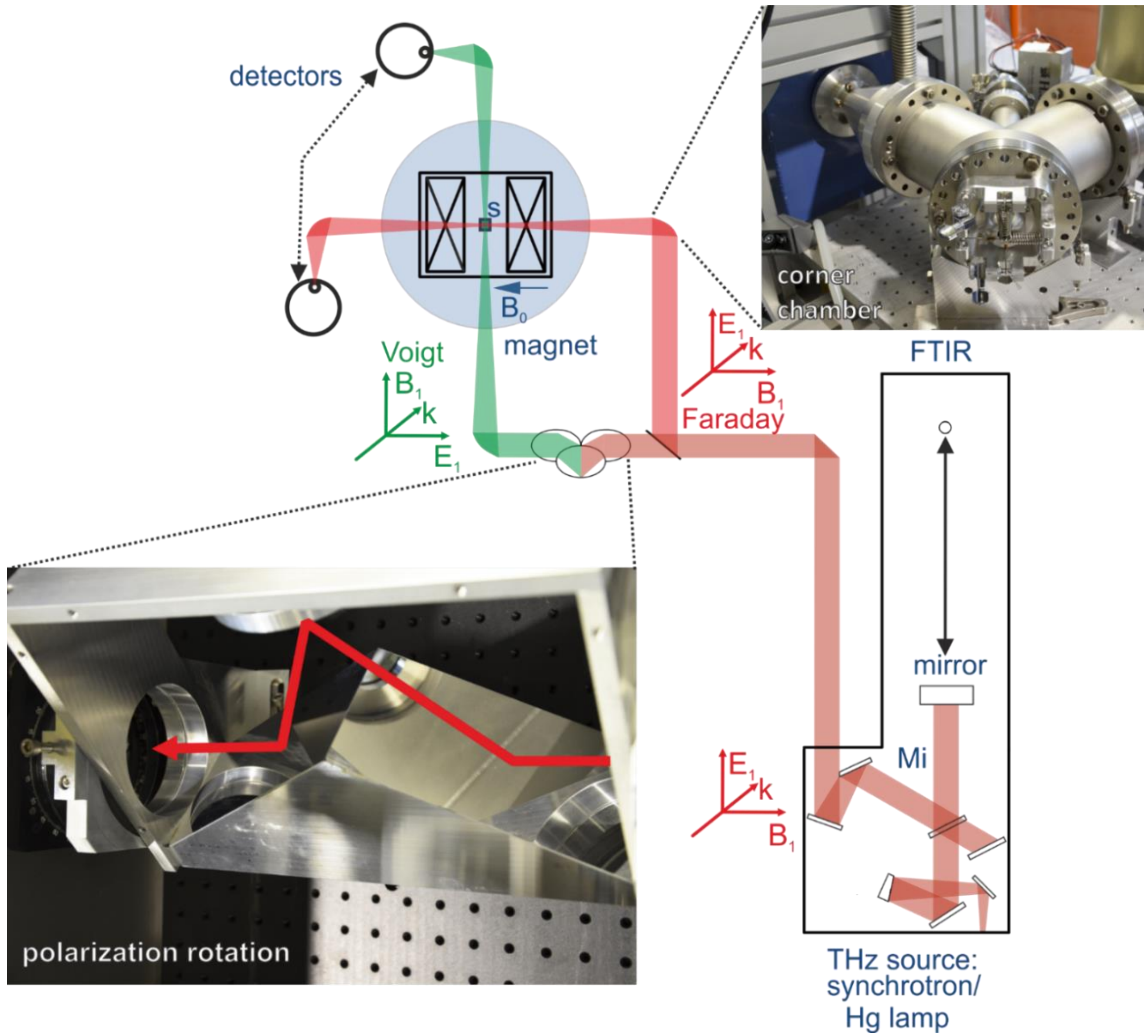

Schnegg, A., ***eMagRes***, *6*, (2017) 115.

FD-FT THz-EPR on Fe^{III} ($S = 5/2$) in Hemin

Frequency Domain Fourier Transform THz-EPR (FD-FT THz-EPR)

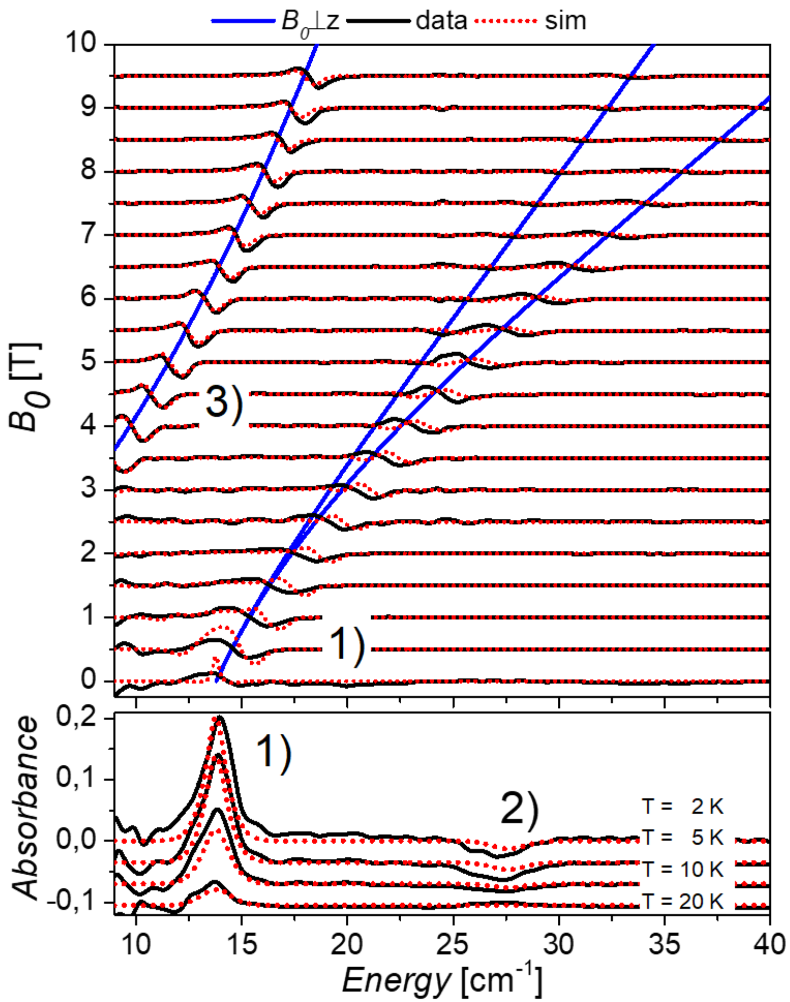

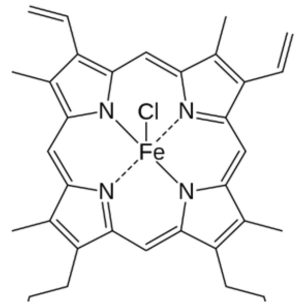

Hemin:
Fe^{III}
$S = 5/2$
D/hc= 6.93 cm^{-1},
$g_\perp$= 1.95, $g_{||}$ = 2.05

$$\hat{H} = D(\hat{S}_z^2 - {}^1/_3 S(S+1)) + \mu_B \boldsymbol{B}_0 \boldsymbol{g} \hat{\boldsymbol{S}}$$

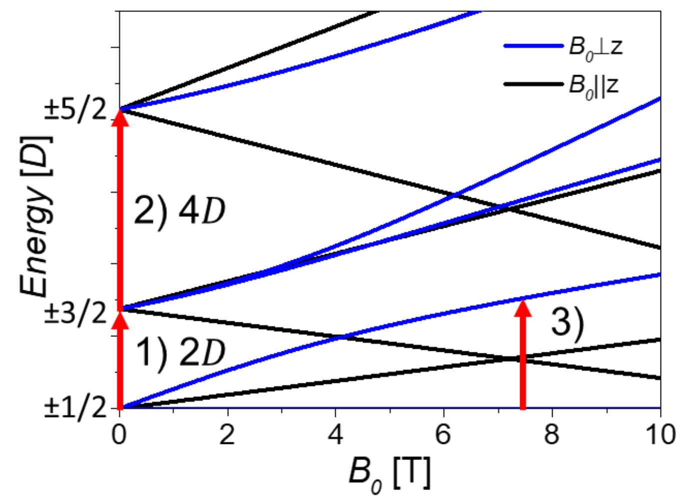

Schnegg A (2017) Very-High-Frequency EPR. *eMagRes*,

Further Reading

Classic:

- A. Abragam, B. Bleaney, Electron paramagnetic resonance of transition ions. Dover: 1986.
- S. A. Al'tshuler, B. M., Kozyrev, Electron paramagnetic resonance in compounds of transition elements. Wiley: 1974.
- J. R. Pilbrow, Transition Ion Electron Paramagnetic Resonance, Oxford: 1990.

Exchange coupled systems:

- A. Bencini, D. Gatteschi, 'EPR of Exchange Coupled Systems', Springer: 1990.

On ZFS:

- J. Telser, Zero Field Splitting, *eMagRes*, 2017, Vol 6: 207–234.

On Very high frequency EPR

- A. Schnegg, ‚Very high frequency EPR', *eMagRes*, 2017, Vol 6: 115–132.